Geophysical Research Letters

RESEARCH LETTER
10.1029/2019GL085897

Key Points:
- Permafrost organic matter derived from coastal erosion dominates nearshore marine sediments
- Nearshore basins trapping sediments in the Arctic Ocean efficiently sequester permafrost organic carbon

Supporting Information:
- Supporting Information S1

Correspondence to:
H. Grotheer,
hendrik.grotheer@awi.de

Citation:
Grotheer, H., Meyer, V., Riedel, T., Pfalz, G., Mathieu, L., Hefter, J., et al. (2020). Burial and origin of permafrost-derived carbon in the nearshore zone of the southern Canadian Beaufort Sea. *Geophysical Research Letters*, *47*, e2019GL085897. https://doi.org/10.1029/2019GL085897

Received 22 OCT 2019
Accepted 22 DEC 2019
Accepted article online 3 JAN 2020

Burial and Origin of Permafrost-Derived Carbon in the Nearshore Zone of the Southern Canadian Beaufort Sea

H. Grotheer[1], V. Meyer[2], T. Riedel[2], G. Pfalz[3], L. Mathieu[1], J. Hefter[1], T. Gentz[1], H. Lantuit[3,4], G. Mollenhauer[1,2], and M. Fritz[3]

[1]Alfred Wegener Institute, Helmholtz Center for Polar and Marine Research, Bremerhaven, Germany, [2]Department of Geosciences and MARUM Centre for Marine Environmental Sciences, University Bremen, Bremen, Germany, [3]Alfred Wegener Institute, Helmholtz Center for Polar and Marine Research, Potsdam, Germany, [4]Institute of Geosciences, Potsdam University, Potsdam, Germany

Abstract Detailed organic geochemical and carbon isotopic ($\delta^{13}C$ and $\Delta^{14}C$) analyses are performed on permafrost deposits affected by coastal erosion (Herschel Island, Canadian Beaufort Sea) and adjacent marine sediments (Herschel Basin) to understand the fate of organic carbon in Arctic nearshore environments. We use an end-member model based on the carbon isotopic composition of bulk organic matter to identify sources of organic carbon. Monte Carlo simulations are applied to quantify the contribution of coastal permafrost erosion to the sedimentary carbon budget. The models suggest that ~40% of all carbon released by local coastal permafrost erosion is efficiently trapped and sequestered in the nearshore zone. This highlights the importance of sedimentary traps in environments such as basins, lagoons, troughs, and canyons for the carbon sequestration in previously poorly investigated, nearshore areas.

Plain Language Summary Increasing air and sea surface temperatures at high latitudes leads to accelerated thaw, destabilization, and erosion of perennially frozen soils (i.e., permafrost), which are often rich in organic carbon. Coastal erosion leads to an increased mobilization of organic carbon into the Arctic Ocean, which there can be converted into greenhouse gases and may therefore contribute to further warming. Carbon decomposition can be limited if organic matter is efficiently deposited on the seafloor, buried in marine sediments, and thus removed from the short-term carbon cycle. Basins, canyons, and troughs near the coastline can serve as sediment traps and potentially accommodate large quantities of organic carbon along the Arctic coast. Here we use biomarkers (source-specific molecules), stable carbon isotopes, and radiocarbon to identify the sources of organic carbon in the nearshore zone of the southern Canadian Beaufort Sea near Herschel Island. We quantify the contribution of coastal permafrost erosion to the sedimentary carbon budget of the area and estimate that more than a third of all carbon released by local permafrost erosion is efficiently trapped in marine sediments. This highlights the importance of regional sediment traps for carbon sequestration.

1. Introduction

Arctic permafrost soils are an important terrestrial carbon reservoir and currently store about 1,300 PgC (Hugelius et al., 2014). Under climate warming scenarios, widespread erosion and thaw of permafrost in the Arctic may lead to massive mobilization of this freeze-locked terrestrial organic carbon (OC_{terr}). As a result, Arctic coastal waters are believed to receive increasing OC_{terr} fluxes from rivers draining permafrost terrain and from eroding permafrost coasts (Fritz et al., 2017). Such increase would result in drastic impacts on global carbon fluxes and their climate feedbacks, on nearshore food webs, and on local communities. However, the fate of the released material in the nearshore zone is quantitatively not well assessed. It may (i) degrade into greenhouse gases (Tanski et al., 2019), (ii) fuel marine primary production, (iii) be buried in nearshore sediments, or (iv) be transported offshore (Fritz et al., 2017; Vonk & Gustafsson, 2013).

Erosion rates along Arctic permafrost coasts, which account for 34% of Earth's coasts (Lantuit et al., 2012), can be as high as 25 m/year (Günther et al., 2015; Jones et al., 2009). Erosion of unconsolidated permafrost soils that can be rich in frozen organic matter (Hugelius et al., 2014; Schuur et al., 2015), results in an annual

release of 4.9–14 Tg of particulate organic carbon (POC) into the nearshore zone (Wegner et al., 2015). This represents more than 4 times the amount of POC contributed by the major Arctic rivers (3.1 Tg; McClelland et al., 2016) and highlights that coastal erosion plays a significant role in the marine carbon budget of the Arctic Ocean. For the southern Canadian Beaufort Sea, Couture et al. (2018) estimated that ~12% of eroded carbon was sequestered in nearshore sediments, whereas Hilton et al. (2015) estimated a significantly higher burial efficiency (~65%) of riverine POC dispatched from the Mackenzie River. Sedimentation rates for the area adjacent to the Mackenzie River range from 2 mm/year near the delta to less than 0.1 mm/year in more distal areas (Harper & Penland, 1982). However, very little information exists on rates of sedimentation and carbon burial for the shelf area to the west of the Mackenzie Delta toward the Yukon-Alaska border. The role of areas with high sediment accumulation such as nearshore basins, troughs, and canyons has not been taken into account in previous studies examining carbon burial rates in this region. OC_{terr} derived from coastal erosion might be substantial in quantity and more bioavailable than riverine and marine OC due to short residence times and high proportions of bioavailable OC in permafrost (Vonk et al., 2012). Thus, the fate of OC_{terr}, its burial rates, origin, age, and vulnerability to decomposition in the nearshore zone remains largely unqualified and uncharacterized.

The aim of this study is to differentiate between marine and several different terrigenous POC sources to elucidate the impact of coastal permafrost erosion and associated POC fluxes on Arctic nearshore sediments. As a case study, we investigate the sources of OC to Herschel Basin, a sedimentary basin situated between Herschel Island and the Mackenzie Delta in the southern Canadian Beaufort Sea (Figure 1). We quantify and characterize OC in nearshore marine surface sediments and a sediment core derived from permafrost coastal erosion, the Mackenzie River, and from autochthonous marine production by using a unique combination of organic geochemical fingerprinting and carbon isotopic composition ($\delta^{13}C$, $\Delta^{14}C$). The carbon isotopic end-member serves to identify the sources of organic carbon and, in combination with Monte Carlo end-member simulations, to quantify the contribution of coastal permafrost erosion to the sedimentary carbon budget.

2. Materials and Methods

2.1. Study Area

The study area exhibits ideal conditions to trace the sources, fluxes, and the fate of OC in the Arctic coastal zone. It features rapidly eroding permafrost coasts with well-defined erosion rates (Couture et al., 2018), a major river discharging into the Arctic Ocean, and a sedimentary basin, serving as a local trap, that receives large amounts of material from both sources on short distances. We focus on rapidly eroding coasts along the Yukon Coastal Plain (YCP) and Herschel Island (69.6°N, 138.9°W) toward the southern Beaufort Sea. Herschel Island is located 3 km offshore between the Alaskan border and the Mackenzie Delta (Figure 1). The island is part of an ice-thrust moraine produced by the northwesternmost advance of the Laurentide Ice Sheet (LIS) during the late Wisconsin (Fritz et al., 2012; Mackay, 1959; Rampton, 1982). The island's coasts are characterized by steep cliffs (up to 50-m high) which are subject to rapid erosion including numerous retrogressive thaw slumps (RTS) and active-layer detachment slides (Lantuit & Pollard, 2008; Obu et al., 2016).

A large sedimentary trap, Herschel Basin (Figure 1), is located to the southeast of Herschel Island and is considered to receive a large portion of the eroded material from Herschel Island and the adjacent mainland coast. The basin covers an area of approximately 126 km^2, with a spatial extent of 7×18 km and maximum water depth of 75 m (O'Connor, 1984). The basin receives material input from (i) coastal erosion, (ii) the Mackenzie River plume and other small rivers (Burn & Zhang, 2009; Forbes, 1981; O'Connor, 1984), and (iii) longshore currents and resulting longshore drift (Figure 1) that are responsible for local sediment and OC transport parallel to the coast (Forbes, 1981; Giovando & Herlinveaux, 1982; Pelletier & Medioli, 2014). The Mackenzie River, however, is commonly considered to be the major fluvial source of sediments and OC to the Canadian Beaufort Shelf region (Hill et al., 1991), including the basin.

2.2. Sampling Locations and Bulk Features

Herschel Island soil samples were collected from two outcrops in 2006, 2009, and 2015. They originate from a 500 m wide RTS located at the southeastern coast (TSD; $n = 4$; Figure 1) and a 150 m wide RTS situated at

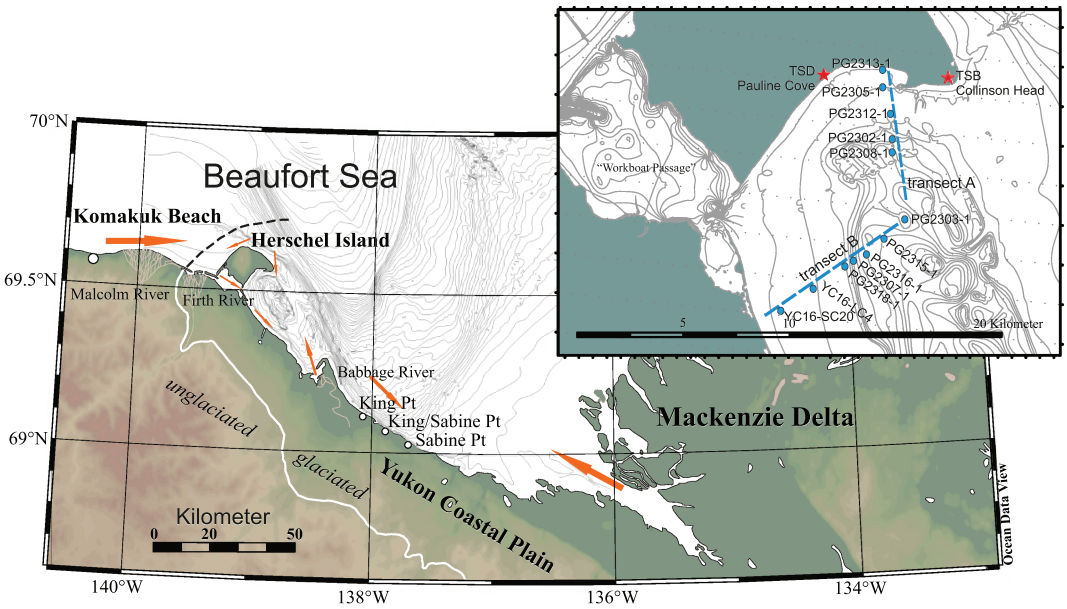

Figure 1. The background map shows the larger sampling area of the Canadian Beaufort Sea. Orange arrows indicate major rivers, currents, and sediment flows toward Herschel Basin (after Pelletier & Medioli, 2014) and white circles indicate sampling locations from Yunker et al. (1992). The solid white line (black dashes) indicates the northwestern most extent of the Laurentide Ice Sheet during the Wisconsin. The small map shows the detailed sampling locations of sediment samples from Herschel Basin (blue circles) and permafrost soils from Herschel Island (red stars).

Collinson Head (TSB; $n = 3$; Figure 1) at the eastern edge of the island. Both locations featured ice-rich permafrost deposits with fine grained sediments and organic carbon contents between 0.6 and 1.8 wt.% (Fritz et al., 2011, 2012). These samples serve as baseline and end-member for the terrestrial coastal environment. Sampling included several stratigraphic layers of the full cliff (up to 20 m height, underneath the active layer) to account for natural biogeochemical variations of the material mobilized by coastal erosion.

Marine surface sediment samples from Herschel Basin (0–1 cm; $n = 12$; collected in 2016) were retrieved along two transects using a gravity corer to ensure undisturbed sediment surfaces. Transect (A) extends in southward direction from Herschel Island to the center of the basin and transect (B) reaches northeastward from the YCP toward the center of the basin (Figure 1). The sediments were of brownish-gray to grayish-black color and consisted of silty to clayey mud. Sediment core PG2303 was collected at the transition of the two transect and had a total length of 12.29 m. The sediment core was retrieved with a UWITEC® piston corer (63 mm PVC liner), which was based on a tripod on the sea ice, and surface sediments were collected with a UWITEC® gravity corer.

All soil and sediment samples were freeze dried, homogenized, and split for subsequent analyses. Full details on biomarker, TOC, stable carbon ($\delta^{13}C_{org}$) and radiocarbon analyses are presented in the supporting information (Text S1).

3. Results and Discussion

Marine Versus Terrigenous Organic Matter—Sterols, GDGTs, and $\delta^{13}C_{org}$

In order to assess the marine versus terrestrial contributions of OC to Herschel Basin the branched and isoprenoid tetraether (BIT) index (Hopmans et al., 2004), the relative abundance of sterols and the stable carbon isotopic composition of bulk OC ($\delta^{13}C_{org}$) were used. The BIT index quantifies the relative abundances of branched glycerol dialkyl glycerol tetraethers (brGDGTs) relative to crenarchaeol (Hopmans et al., 2004). brGDGTs are very abundant in various terrestrial settings including mineral soils, peats, lakes, and rivers (Blaga et al., 2010; De Jonge et al., 2014, 2015; Weijers et al., 2007). By contrast, crenarchaeol is dominantly produced by marine Thaumarchaeota (e.g., Schouten et al., 2013, and references therein). The BIT index can be applied to estimate the relative contributions of marine and terrestrial organic matter in marine sediments. An index value of around 1 indicates the predominance of brGDGTs pointing to relatively high

terrigenous influence, whereas a value near 0 is typical of offshore marine settings (De Jonge et al., 2015; Sinninghe Damsté, 2016; Warden et al., 2016). Likewise, the fractional abundances of β-sitosterol, brassicasterol, and dinosterol can be used to estimate the OC origin (e.g., Fahl & Stein, 2007, 2012; Hörner et al., 2016). While β-sitosterol is synthesized by vascular plants (e.g., Volkman, 1986; Yunker et al., 1995), brassicasterol and dinosterol are produced by marine algae and dinoflagellates (e.g., Volkman, 2016). The fractional abundance of β-sitosterol ($f_{\beta\text{-sitosterol}}$) hence also serves as a measure to estimate the relative contribution of terrestrial to marine OC. $f_{\beta\text{-sitosterol}}$ was calculated as follows (β-sitosterol/(β-sitosterol + brassicasterol + dinosterol)). Values near 1 indicate the predominance of terrigenous β-sitosterol and a value of 0 pointing to full marine conditions.

Herschel Basin surface sediments are dominated by terrestrial OC as inferred from the relatively high $f_{\beta\text{-sitosterol}}$ and BIT index (0.7 ± 0.1 [mean ± S.D.] and 0.8 ± 0.1). They show no trends along the two transects, suggesting uniformly high and widespread contribution of terrestrial OC to nearshore sediments (Figures 2a and 2b and Table S1). This is further supported by the $\delta^{13}C_{org}$ being remarkably consistent (−26.2‰ ± 0.3‰) across the transects and within the range of previously published values for near shore sediments and onshore soils in this area (Couture et al., 2018; Fritz et al., 2012).

Herschel Island soils are more heterogeneous than the surface sediments. The $f_{\beta\text{-sitosterol}}$ varies between 0.24 and 0.86 (0.7 ± 0.3) and the BIT index between 0.51 and 0.98 (0.9 ± 0.2). The majority of samples show a predominance of β-sitosterol (four out of six samples) and brGDGTs (five out of seven) pointing to a terrestrial origin of the OC. However, two samples from the Collision Head RTS show higher contributions of the marine compounds (i.e., crenarchaeol, brassicasterol, and dinosterol; Table S1). Hydrochemical signatures of massive ground ice bodies on Herschel Island suggest that the island consists of upthrusted nearshore sediments deposited during the Late Wisconsin advance of the LIS (Fritz et al., 2011, 2012). This is in good agreement with bulk organic radiocarbon ages of ~25 ± 6 kyr BP ($F^{14}C_{org}$ = 0.056 ± 0.041; Figure 2d and Table S1) obtained from our sampling sites on Herschel Island. The contribution of allochthonous marine sediments to the deposits on Herschel Island might explain the relatively high abundance of marine biomarkers in these two outcrop samples. Perennially frozen conditions suppressed microbial degradation of OC in Herschel Island soils and leading to accumulation and preservation of several millennia old OC, as observed widely in permafrost regions in Siberia and Alaska (Strauss et al., 2017). Further, the organic geochemical composition (high BIT and $f_{\beta\text{-sitosterol}}$) of the soils suggest that the pre-glacial sediments that later formed Herschel Island were also dominated by terrestrial OC comparable to the current regional setting. Thus, the mixture of allochthonous and autochthonous sediments on Herschel Island explains the heterogeneity of the biomarker distribution observed in our data set.

Origin of OC in Herschel Basin—Hopanoids and Radiocarbon Ages

The hopane composition and radiocarbon ages show distinct differences between terrestrial soils on Herschel Island and marine sediments from the basin. Radiocarbon ages of soil bulk OC (25 ± 6 kyr BP) are older than the basin sediments (11 ± 2 kyr BP). Samples from the center of the basin and closest to Herschel Island are the oldest, whereas the youngest samples are located close to the mainland of the YCP (Figure 2d). This is in good agreement with lower cliff heights and thus higher volumes of younger material eroded along the mainland coast (Couture et al., 2018) in contrast to Herschel Island. Herschel Island soils are dominated by the C_{30}αβ-hopane and C_{29}αβ-norhopane thermodynamically and geologically stable hopane stereoisomers. These are degradation products of "biological" ββ-hopanoids (Peters & Moldowan, 1991) which are synthesized by bacteria (Rohmer et al., 1984). Similar to Herschel Island soils, geological C_{30}αβ-hopane and C_{29}αβ-norhopane are abundant in Herschel Basin sediments, but these samples are additionally characterized by high abundances of the biological diploptene (C_{30}ββ-hopene). Whereas the C_{30}αβ-hopane and C_{29}αβ-norhopane show high relative abundances consistently throughout the sample set (i.e., Herschel Basin and Herschel Island), the relative abundance of diploptene shows a large variability relative to these two compounds, particularly across the basin (Figure 2c and Table S1). Therefore, the ratio of diploptene to the sum of diploptene, C_{29}αβ-norhopane, and C_{30}αβ-hopane (hereafter referred to as diploptene-ratio) can be used to identify different clusters within the sample set and is suitable to characterize the molecular fingerprint of Herschel Island soils and Herschel Basin sediments. The diploptene-ratio ranges between 0.3 and 0.7 (0.4 ± 0.2) in Herschel Basin sediments and 0.0–0.3 (0.2 ± 0.1) in Herschel Island soils (Figure 2c and Table S1) and hence discriminates Herschel Island soils from Herschel Basin sediments

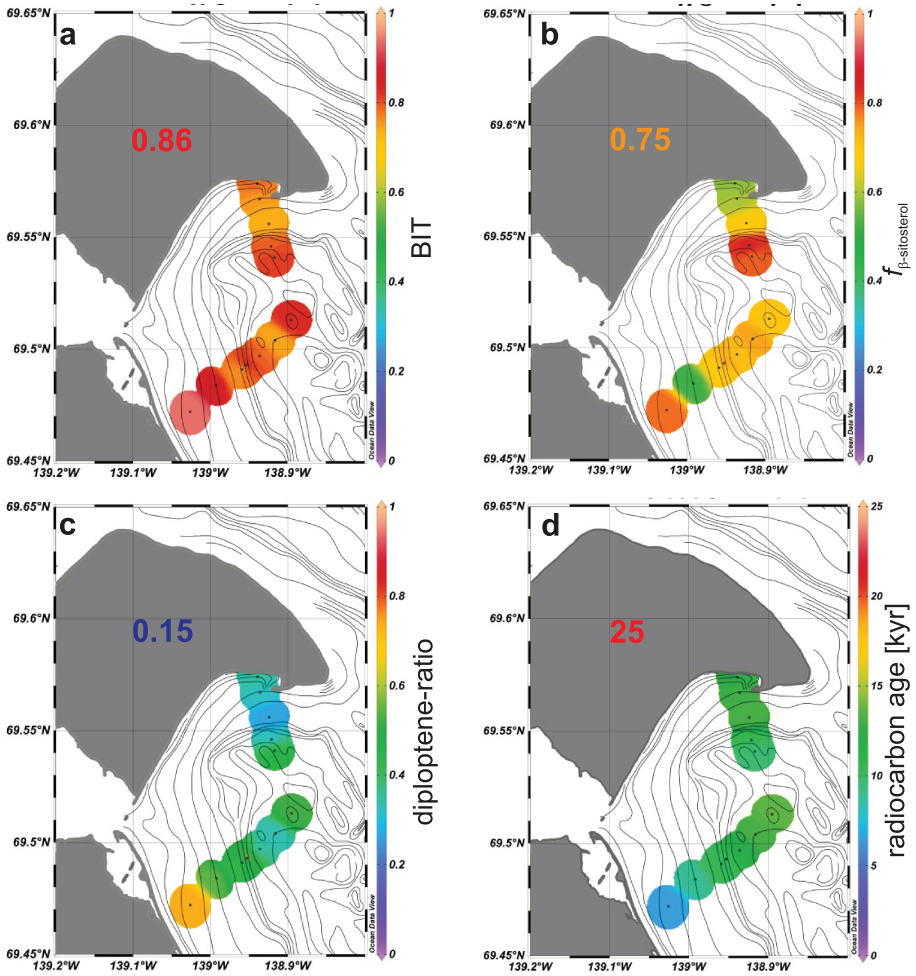

Figure 2. Surface maps of organic geochemical parameters. The color code refers to single measurements of each surface sediment sample ($n = 12$). The number in the center of the island represents the average value of all soil samples ($n = 7$). (a) BIT index (Hopmans et al., 2004); (b) $f_{\beta\text{-sitosterol}}$ = β-sitosterol/(β-sitosterol + brassicasterol + dinosterol); (c) diploptene-ratio = diploptene/(diploptene + C_{29}αβ-norhopane + C_{30}αβ-hopane); and (d) conventional radiocarbon age of bulk OM in kyr BP.

(independent *t* test *p* value << 0.05). The highest relative diploptene content was present closest to the YCP, whereas the lowest content was detected directly off Herschel Island.

The spatial distributions of radiocarbon ages and diploptene ratios are potentially related to each other as diploptene contents decrease with increasing age (Figure S1). The oldest radiocarbon ages are found directly off Herschel Island while the youngest material was deposited close to the YCP. The basin receives a mixture of OC from coastal erosion on Herschel Island (older, low diploptene content) and from additional sources that provide younger, diploptene-rich OC ($R^2 = 0.7$, *p* value << 0.05; Figure S1). The BIT and $f_{\beta\text{-sitosterol}}$ suggest that marine OC contribution is limited, and the major additional sources of OC are terrestrial. Diploptene was shown to be formed by soil dwelling bacteria and is vastly abundant in coastal peats along the YCP and POC from the Mackenzie River (Yunker et al., 1992, 1993). Hence, the most likely additional sources of terrigenous OC are coastal erosion from the YCP (Couture et al., 2018) and fluvial discharge from the Mackenzie River (Drenzek et al., 2007; Macdonald et al., 1998; Yunker et al., 1993). Yunker et al. (1993) report high diploptene concentrations in POC samples from the Mackenzie River retrieved before freshet (April to May); however, with increasing sediment load during and after freshet (September), the relative diploptene content decreased. Before freshet, the hopanes are sourced from local YCP peats (dominated by biologically produced diploptene, lean in diagenetic C_{30}αβ-hopane, and C_{29}αβ-norhopane) within the catchment of the delta, whereas later, during freshet, the relative abundance of petrogenic material

(including $C_{30}\alpha\beta$-hopane and $C_{29}\alpha\beta$-norhopane) increases (Yunker et al., 1993). The petrogenic contribution is presumably derived from the Devonian Canol formation in the Mackenzie River hinterland (Yunker et al., 2002). However, the diploptene ratios of Mackenzie Delta POC (0.5 ± 0.1) and shelf POC (0.8 ± 0.1) vary significantly and show that the relative diploptene content increases from the center of the delta toward the shelf edge (Yunker et al., 1992, 1993). This implies significant contribution of eroded coastal peats (diploptene ratio 1 ± 0.1; Table S3), to the shelf POC. Mackenzie River POC shows a mixture of fresh biologic diploptene and, depending on the season, increased contents of petrogenic hopanes from the Canol formation (Yunker et al., 2002). The ternary plot (Figure S2) shows the relative abundances of diploptene, $C_{30}\alpha\beta$-hopane, and $C_{29}\alpha\beta$-norhopane. Whereas the Herschel Island samples, summarized as the Herschel Island soil end-member, are enriched in diagenetic hopanes; the YCP peat end-member is highly enriched in diploptene and depleted in diagenetic hopanes. The Herschel Basin sediments plot along a mixing line between the two end-members, suggesting varying contribution of freshly eroded coastal peats and eroded Herschel Island soils. However, due to ill-constrained and highly variable diploptene-ratios for Mackenzie POC (Figure S2), the hopanoid distribution does not allow a quantitative source apportionment for the basin sediments. Nevertheless, they point toward a complex mixing and efficient trapping of OC originating from terrestrial sources.

3.2. Source Apportionment

In order to identify potential contributions from the Mackenzie River and the YCP, our data from Herschel Island and Herschel Basin are compared to the carbon isotopic composition of POC from the Mackenzie River. The stable carbon isotopic composition of Mackenzie River POC ($\delta^{13}C_{MackenziePOC}$) was obtained from the literature on samples collected between March and September in 2004 and 2005 (Guo et al., 2007; Holmes et al., 2018). It varies significantly and is independent of sampling location and time of the year. The $\delta^{13}C_{MackenziePOC}$ ranges between −30.8‰ and −22.1‰ ($\delta^{13}C_{MackenziePOC}$ = -28.3‰ ± 2.4‰; Table S2) and on average is slightly depleted relative to Herschel Island soils and Herschel Basin sediment. With an average of ~6.6 ± 1.2 kyr ($F^{14}C_{MackenziePOC}$ = 0.441 ± 0.066; Table S2), Mackenzie River POC, shown to be derived primarily from top-soil permafrost thaw and riverbank erosion in the catchment (Guo et al., 2007), is significantly younger than Herschel Island soils.

The isotopic composition separates the OC sources (i.e., Mackenzie River POC, marine POC and Herschel Island soil OC) nicely in a dual-carbon isotope plot (Figure 3a). Therefore, we estimate the carbon isotopic end-member composition of Mackenzie and Herschel Island based on the mean $\delta^{13}C$ and $F^{14}C$ values. Due to the absence of appropriate data, no isotopic end-member for the YCP can be defined, and marine $\delta^{13}C_{POC}$ varies widely in Arctic waters (Vonk et al., 2012, and references within). As no data constraining the carbon isotopic composition of local phytoplankton is available for the basin the $\delta^{13}C_{marinePOC}$ value (−24‰ ± 1‰) proposed by Vonk et al. (2014) and the estimated reservoir age (1.1 kyr; $F^{14}C_{marinePOC}$ = 0.872 ± 0.011; Text S2) were used to define the marine POC end-member. Herschel Basin sediments plot within a mixing triangle between the two terrestrial OC end-members and with limited contribution of marine POC, in line with the findings from the BIT index and $f_{\beta\text{-sitosterol}}$ elaborated above.

The relative contribution of sources to the basin sediments was calculated by end-member mixing analysis using Monte Carlo Simulations. This approach was previously used for source apportionment calculations in Arctic sediments (e.g., Karlsson et al., 2011; Vonk et al., 2012, 2014). The model was described in detail by Andersson (2011) and Sheesley et al. (2011) and allows to account for end-member variability. The bulk organic carbon isotopic composition ($\delta^{13}C$ and $F^{14}C$) allows to construct an end-member mixing model to calculate the contribution/fraction of Herschel Island eroded OC to the basin sediments ($f_{Herschel\ Island}$). The end-member values of marine POC, Herschel Island soil and Mackenzie River POC were defined above.

The contribution of eroded Herschel Island soil OC ($f_{\ Herschel\ Island}$) to the sediments are shown in Figure 3b and Table S4. The model suggests lowest contribution of Herschel Island OC to sediments closest to the YCP and highest contribution to sediments closest to Herschel Island and toward the center of the basin. However, the model does not account for the contribution of coastal peats (due to the lack of data).

3.3. Central Basin Sediment Core

Based on radiocarbon dates of marine mollusks (Text S2) the 12.3 m long sediment core PG2303 covers the last ~4,000 years (Text S2, Figure S4, and Table S5). This equates to an average annual sedimentation rate of

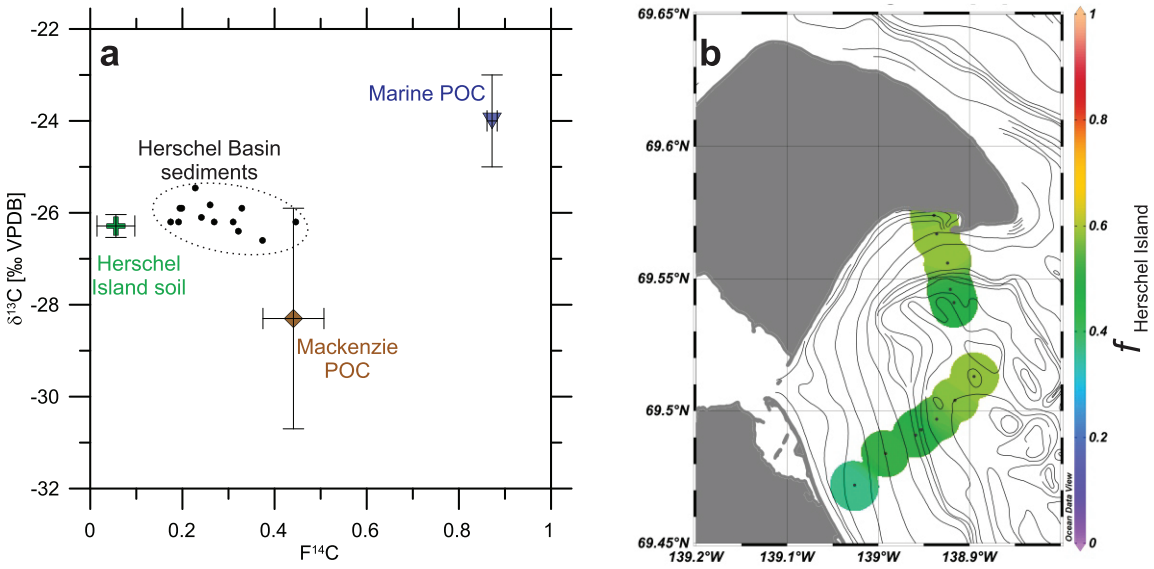

Figure 3. End-member model and resulting source apportionment surface maps. (a) Dual carbon isotope plot illustrating data used for Monte Carlo Simulation. End-members for Herschel Island (green), Mackenzie River POC (brown), and marine POC (blue). Basin sediments (black) plot along a mixing triangle between all three sources. (b) Surface map of calculated fractional abundance of OM sourced from Herschel Island to the surface samples ($n = 12$) based on the dual-carbon isotope end-member model.

0.33 cm/year in the center of the basin. The sedimentation rate, TOC content (1.8 ± 0.1 wt.%) and $\delta^{13}C_{org}$ (−26.2‰ ± 0.1‰) were stable over time (Figure 4 and Table S6), although TOC slightly decreased for the last 500 years. The organic geochemical proxies also show no significant variation with depth and time. BIT index and $f_{\beta\text{-sitosterol}}$ indicate that the marine sediments were dominated by terrestrial inputs and $F^{14}C_{org}$ suggests that the terrestrial OM was preaged prior to deposition. The calculated contribution of Herschel Island derived OC ($f_{\text{Herschel Island}}$) to the basin was also constant through time, suggesting very stable conditions and sedimentation patterns.

However, one noticeable event horizon can be identified ~650 year BP, where for a short period more and younger terrestrial OC was deposited in the basin. The increase in diploptene ratio alongside a decrease in OC derived from Herschel Island suggests increased contribution of coastal peats and/or Mackenzie river run-off. During the late Holocene northern Canada was subject to periodically colder climatic conditions (O'Brien et al., 1995) corresponding with glacier advances in the St. Elias Mountains (southern Yukon Territory; Denton & Karlén, 1973) that could cause increased river discharge and hence erosion of coastal

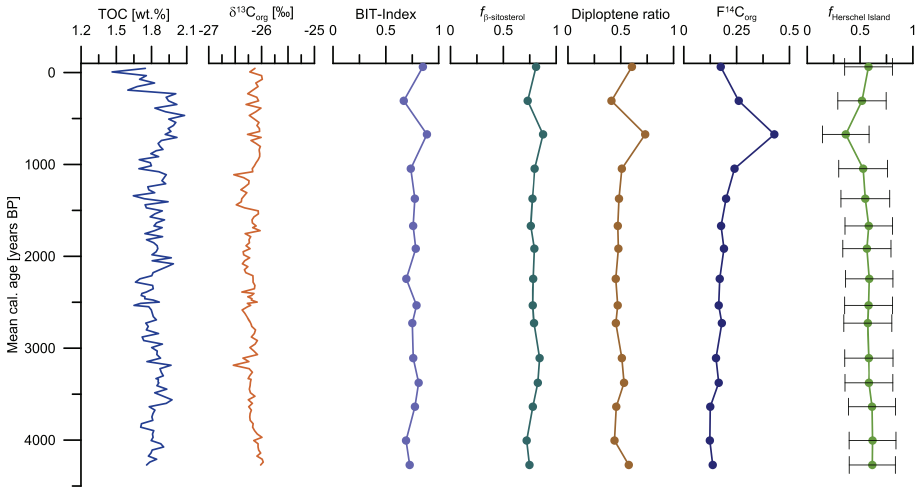

Figure 4. Organic geochemical results for the sediment core PG2303 retrieved from the center of Herschel Basin.

peats. The timing of fluctuation coincides broadly with the Little Ice Age cooling (ca. 1400–1850 AD; Campbell et al., 1998), suggesting a response to the short-term cooling and thus confirming the sensitivity of the applied methods and model to changing environmental conditions. However, the exact mechanism behind the anomaly cannot be identified. An increase in river discharge due to glacial runoff would increase the inorganic clastic sediment supply, which would potentially lead to a, not observed, dilution of the TOC content. Unfortunately, the sampling resolution is insufficient to identify any anthropogenically induced changes in sedimentation patterns over the last ~150 years.

3.4. Carbon Burial in the Basin Sediments

The model results, based on the surface samples, suggest that 56% ± 6% of OC in basin sediments originates from coastal erosion on Herschel Island. For a first-order estimation of the burial of organic carbon from coastal erosion, we extrapolate these observations to the entire basin assuming homogenous stratigraphy and sedimentation rates across the entire basin. With an average sediment density of 1,700 kg/m^3 over an area of 127 km^2, the basin receives approximately 720,000 t/year of sediment. Considering an average TOC content of 1.2 wt.%, that includes all surface sediment samples used in this study, the basin accumulates ~8,600 tC/year from different sources. Couture et al. (2018) estimated that Herschel Island loses ~12,000 tC/year due to coastal retreat. From the present calculations the basin accumulates ~4,800 tC/year from Herschel Island, which converts into ~40% of the eroded carbon from the island. The remaining 60% are likely transported elsewhere on the shelf, offshore, or are at least partially remineralized by microbial decomposition in the water column (de Haas et al., 2002; Hedges et al., 1997). This estimation should be considered as a maximum value for OC eroded from Herschel Island itself, as any potential contribution of OC originating from the YCP cannot be accounted for due to the lack of YCP soil data.

The results on OC burial obtained here (~40%) suggest substantially higher sequestration rates compared to previous estimates (~12%) of eroded OC for the entire Yukon coastal shelf (Couture et al., 2018) but lower rates (~65%) for particulate OC delivered by the Mackenzie River (Hilton et al., 2015). Hilton et al. (2015), Couture et al. (2018), and this study applied different methodological and conceptual approaches to estimate the burial efficiency of OC and thus results may not be directly comparable. Data from Hilton et al. (2015) would suggest that riverine POC is more efficiently buried, whereas OC eroded from the coast may be preferentially mineralized and, thus, has a potentially stronger influence on greenhouse gas emissions. This observation questions the traditional paradigm that rivers transport the "fresher" biospheric OC into the Arctic Ocean. Apparently, permafrost contains a large reservoir of easily degradable OC (Vonk et al., 2013) even if this OC is old, but it has been kept freeze-locked and undegraded for millennia. This apparent mismatch highlights the need for intermethodological comparison studies to improve the reliability and validity of estimated OC burial rates.

Previous results from the Laptev Sea showed that a large percentage of carbon contained in sediments of the inner shelf originates from erosion of the shelf itself (Vonk et al., 2012) and is further deposited on the outer shelf (Wegner et al., 2015). Studies in the Beaufort Sea (this study, Couture et al., 2018; Hilton et al., 2015) highlight depositional environments, where carbon may be stored on long time scales, are actually conceivably close to shore. This study highlights the crucial role of sedimentary traps such as basins, lagoons, troughs, and canyons for carbon sequestration in the nearshore zone. As such, these systems may act as important sinks for organic carbon mobilized during permafrost thaw and erosion along coastlines associated with future warming.

Acknowledgments
We wish to express our thanks to the Yukon Territorial Government and the Yukon Parks (Herschel Island Qiqiktaruk Territorial Park). The authors acknowledge the support of the Aurora Research Institute (ARI, Inuvik) for the field component. MF was supported by the Daimler and Benz Foundation (grant 32-02/15). Field support was provided by George Tanski, Jan Kahl, Boris Biskaborn, Samuel McLeod, and Edward McLeod. Elizabeth Bonk provided analytical support at AWI. This project has received funding from European Union Framework Programme for Research and Innovation - Horizon 2020 (grand agreement number 773421; project: NUNATARYUK)). We want to thank the three anonymous reviewers and Editor Rose Cory for their helpful and constructive comments that helped improving the manuscript. Data can be accessed via PANGAEA https://doi.pangaea.de/10.1594/PANGAEA.910013.

References

Andersson, A. (2011). A systematic examination of a random sampling strategy for source apportionment calculations. *Science of the Total Environment*, *412–413*, 232–238.

Blaga, C. I., Reichart, G. J., Schouten, S., Lotter, A. F., Werne, J. P., Kosten, S., et al. (2010). Branched glycerol dialkyl glycerol tetraethers in lake sediments: Can they be used as temperature and pH proxies? *Organic Geochemistry*, *41*(11), 1225–1234. https://doi.org/10.1016/j.orggeochem.2010.07.002

Burn, C. R., & Zhang, Y. (2009). Permafrost and climate change at Herschel Island (Qikiqtaruq), Yukon Territory, Canada. *Journal of Geophysical Research*, *114*, F02001. https://doi.org/10.1029/2008JF001087

Campbell, I. D., Campbell, C., Apps, M. J., Rutter, N. W., & Bush, A. B. G. (1998). Late Holocene ~1,500 yr climatic periodicities and their implications. *Geology*, *26*(5), 471–473.

Couture, N. J., Irrgang, A., Pollard, W., Lantuit, H., & Fritz, M. (2018). Coastal erosion of permafrost soils along the Yukon Coastal Plain and fluxes of organic carbon to the Canadian Beaufort Sea. *Journal of Geophysical Research: Biogeosciences*, *123*, 406–422. https://doi.org/10.1002/2017JG004166

de Haas, H., van Weering, T. C. E., & de Stigter, H. (2002). Organic carbon in shelf seas: sinks or sources, processes and products. *Continental Shelf Research*, *22*, 691–717.

De Jonge, C., Hopmans, E. C., Zell, C. I., Kim, J. H., Schouten, S., & Sinninghe Damsté, J. S. (2014). Occurrence and abundance of 6-methyl branched glycerol dialkyl glycerol tetraethers in soils: Implications for paleoclimate reconstruction. *Geochimica et Cosmochimica Acta*, *141*, 97–112.

De Jonge, C., Stadnitskaia, A., Hopmans, E. C., Cherkashov, G., Fedotov, A., Streletskaya, I. D., et al. (2015). Drastic changes in the distribution of branched tetraether lipids in suspended matter and sediments from the Yenisei River and Kara Sea (Siberia): Implications for the use of brGDGT-based proxies in coastal marine sediments. *Geochimica et Cosmochimica Acta*, *165*, 200–225. https://doi.org/10.1016/j.gca.2015.05.044

Denton, G. H., & Karlén, W. (1973). Holocene climatic variations—Their pattern and possible cause. *Quaternary Research*, *3*(2), 155–205.

Drenzek, N. J., Montluçon, D. B., Yunker, M. B., Macdonald, R. W., & Eglinton, T. I. (2007). Constraints on the origin of sedimentary organic carbon in the Beaufort Sea from coupled molecular ^{13}C and ^{14}C measurements. *Marine Chemistry*, *103*(1–2), 146–162.

Fahl, K., & Stein, R. (2007). Biomarker records, organic carbon accumulation, and river discharge in the Holocene southern Kara Sea (Arctic Ocean). *Geo-Marine Letters*, *27*(1), 13–25.

Fahl, K., & Stein, R. (2012). Modern seasonal variability and deglacial/Holocene change of central Arctic Ocean sea-ice cover: New insights from biomarker proxy records. *Earth and Planetary Science Letters*, *351–352*, 123–133.

Forbes, D. L. (1981). Babbage River delta and lagoon: Hydrology and sedimentology of an Arctic estuarine system. University of British Columbia.

Fritz, M., Vonk, J. E., & Lantuit, H. (2017). Collapsing Arctic coastlines. *Nature Climate Change*, *7*(1), 6–7. https://doi.org/10.1038/nclimate3188

Fritz, M., Wetterich, S., Meyer, H., Schirrmeister, L., Lantuit, H., & Pollard, W. H. (2011). Origin and characteristics of massive ground ice on Herschel Island (western Canadian Arctic) as revealed by stable water isotope and Hydrochemical signatures. *Permafrost and Periglacial Processes*, *22*(1), 26–38. https://doi.org/10.1002/ppp.714

Fritz, M., Wetterich, S., Schirrmeister, L., Meyer, H., Lantuit, H., Preusser, F., & Pollard, W. H. (2012). Eastern Beringia and beyond: Late Wisconsinan and Holocene landscape dynamics along the Yukon Coastal Plain, Canada. *Palaeogeography, Palaeoclimatology, Palaeoecology*, *319–320*, 28–45. https://doi.org/10.1016/j.palaeo.2011.12.015

Giovando, L. F., & Herlinveaux, R. H. (1982). A discussion of factors influencing the dispersion of pollutants in the Beaufort Sea. *Pacific Marine Science Reports*, *81*(4).

Günther, F., Overduin, P. P., Yakshina, I. A., Opel, T., Baranskaya, A. V., & Grigoriev, M. N. (2015). Observing Muostakh disappear: Permafrost thaw subsidence and erosion of a ground-ice-rich Island in response to arctic summer warming and sea ice reduction. *The Cryosphere*, *9*(1), 151–178.

Harper, J. R., & Penland, P. S. (1982). *Beaufort Sea sediment dynamics, Contract report to Atlantic Geoscience Centre*. Ottawa, ON: Geological Survey of Canada.

Hedges, J. I., Keil, R. G., & Benner, R. (1997). What happens to terrestrial organic matter in the ocean? *Organic Geochemistry*, *27*(5–6), 195–212.

Hill, P. R., Blasco, S. M., Harper, J. R., & Fissel, D. B. (1991). Sedimentation on the Canadian Beaufort Shelf. *Continental Shelf Research*, *11*(8-10), 821–842. https://doi.org/10.1016/0278-4343(91)90081-G

Hilton, R. G., Galy, V., Gaillardet, J., Dellinger, M., Bryant, C., O'Regan, M., et al. (2015). Erosion of organic carbon in the Arctic as a geological carbon dioxide sink. *Nature*, *524*(7563), 84–87. https://doi.org/10.1038/nature14653

Hörner, T., Stein, R., Fahl, K., & Birgel, D. (2016). Post-glacial variability of sea ice cover, river run-off and biological production in the western Laptev Sea (Arctic Ocean) - A high-resolution biomarker study. *Quaternary Science Reviews*, *143*, 133–149.

Hugelius, G., Strauss, J., Zubrzycki, S., Harden, J. W., Schuur, E. A. G., Ping, C. L., et al. (2014). Estimated stocks of circumpolar permafrost carbon with quantified uncertainty ranges and identified data gaps. *Biogeosciences*, *11*(23), 6573–6593. https://doi.org/10.5194/bg-11-6573-2014

Jones, B. M., Arp, C. D., Jorgenson, M. T., Hinkel, K. M., Schmutz, J. A., & Flint, P. L. (2009). Increase in the rate and uniformity of coastline erosion in Arctic Alaska. *Geophysical Research Letters*, *36*, L03503. https://doi.org/10.1029/2008GL036205

Karlsson, E. S., Charkin, A., Dudarev, O., Semiletov, I., Vonk, J. E., Sánchez-García, L., & Andersson, A. (2011). Carbon isotopes and lipid biomarker investigation of sources, transport and degradation of terrestrial organic matter in the Buor-Khaya Bay, SE Laptev Sea. *Biogeosciences*, *8*(7), 1865–1879.

Lantuit, H., Overduin, P. P., Couture, N., Wetterich, S., Aré, F., Atkinson, D., et al. (2012). The Arctic coastal dynamics database: A new classification scheme and statistics on Arctic permafrost coastlines. *Estuaries and Coasts*, *35*(2), 383–400. https://doi.org/10.1007/s12237-010-9362-6

Lantuit, H., & Pollard, W. H. (2008). Fifty years of coastal erosion and retrogressive thaw slump activity on Herschel Island, southern Beaufort Sea, Yukon Territory, Canada. *Geomorphology*, *95*(1–2), 84–102. https://doi.org/10.1016/j.geomorph.2006.07.040

Macdonald, R. W., Solomon, S. M., Cranston, R. E., Welch, H. E., Yunker, M. B., & Gobeil, C. (1998). A sediment and organic carbon budget for the Canadian Beaufort shelf. *Marine Geology*, *144*(4), 255–273.

Mackay, J. R. (1959). Glacier ice-thrust features of the Yukon Coast. *Geographical Bulletin*, *13*, 5–21.

McClelland, J. W., Holmes, R. M., Peterson, B. J., Raymond, P. A., Striegl, R. G., Zhulidov, A. V., et al. (2016). Particulate organic carbon and nitrogen export from major Arctic rivers. *Global Biogeochemical Cycles*, *30*, 629–643. https://doi.org/10.1002/2015GB005351

O'Brien, S. R., Mayewski, P. A., Meeker, L. D., Meese, D. A., Twickler, M. S., & Whitlow, S. (1995). Reconstructed from a Greenland Ice Core. *Science*, *270*(21), 1962–1964.

Obu, J., Lantuit, H., Fritz, M., Pollard, W. H., Sachs, T., & Günther, F. (2016). Relation between planimetric and volumetric measurements of permafrost coast erosion: A case study from Herschel Island, western Canadian Arctic. *Polar Research*, *35*(1), 30313. https://doi.org/10.3402/polar.v35.30313

O'Connor, M. J. (1984). Surficial geology and granular resources southeast of Herschel Island.

Pelletier, B. R., & Medioli, B. E. (2014). Environmental Atlas of the Beaufort Coastlands. In *Geological Survey of Canada, Open File 7619*.

Peters, K. E., & Moldowan, J. M. (1991). Effects of source, thermal maturity, and biodegradation on the distribution and isomerization of homohopanes in petroleum. *Organic Geochemistry*, *17*(1), 47–61. https://doi.org/10.1016/0146-6380(91)90039-M

Rampton, V. N. (1982). Quaternary geology of the Yukon Coastal Plain. *Geological Survey of Canada Bulletin*, *317*.

Rohmer, M., Bouvier-Nave, P., & Ourisson, G. (1984). Distribution of hopanoid triterpenes in prokaryotes. *Journal of General Microbiology*, *130*, 1137–1150.

Schuur, E. A. G., McGuire, A. D., Schädel, C., Grosse, G., Harden, J. W., Hayes, D. J., et al. (2015). Climate change and the permafrost carbon feedback. *Nature*, *520*(7546), 171–179. https://doi.org/10.1038/nature14338

Sheesley, R. J., Andersson, A., & Gustafsson, Ö. (2011). Source characterization of organic aerosols using Monte Carlo source apportionment of PAHs at two South Asian receptor sites. *Atmospheric Environment*, *45*(23), 3874–3881.

Sinninghe Damsté, J. S. (2016). Spatial heterogeneity of sources of branched tetraethers in shelf systems: The geochemistry of tetraethers in the Berau River delta (Kalimantan, Indonesia). *Geochimica et Cosmochimica Acta*, *186*, 13–31.

Strauss, J., Schirrmeister, L., Grosse, G., Fortier, D., Hugelius, G., Knoblauch, C., et al. (2017). Deep Yedoma permafrost: A synthesis of depositional characteristics and carbon vulnerability. *Earth-Science Reviews*, *172*(July), 75–86. https://doi.org/10.1016/j.earscirev.2017.07.007

Tanski, G., Wagner, D., Knoblauch, C., Fritz, M., Sachs, T., & Lantuit, H. (2019). Rapid CO_2 release from eroding permafrost in seawater. *Geophysical Research Letters*, *46*, 244–252. https://doi.org/10.1029/2019GL084303

Volkman, J. K. (1986). A review of sterol markers for marine and terrigenous organic matter. *Organic Geochemistry*, *9*(2), 83–99.

Volkman, J. K. (2016). Sterols in Microalgae. In M. Borowitzka, J. Beardall, & J. Raven (Eds.), *The physiology of microalgae. Developments in Applied Phycology* (Vol. 6, pp. 485–505). Cham, Switzerland: Springer.

Vonk, J. E., & Gustafsson, Ö. (2013). Permafrost-carbon complexities. *Nature Geoscience*, *6*(9), 675–676.

Vonk, J. E., Mann, P. J., Davydov, S., Davydova, A., Spencer, R. G. M., Schade, J., et al. (2013). High biolability of ancient permafrost carbon upon thaw. *Geophysical Research Letters*, *40*(11), 2689–2693. https://doi.org/10.1002/grl.50348

Vonk, J. E., Sánchez-García, L., van Dongen, B. E., Alling, V., Kosmach, D., Charkin, A., et al. (2012). Activation of old carbon by erosion of coastal and subsea permafrost in Arctic Siberia. *Nature*, *489*(7414), 137–140. https://doi.org/10.1038/nature11392

Vonk, J. E., Semiletov, I. P., Dudarev, O. V., Eglinton, T. I., Andersson, A., Shakhova, N., et al. (2014). Preferential burial of permafrost-derived organic carbon in Siberian-Arctic shelf waters. *Journal of Geophysical Research: Oceans*, *119*, 8410–8421. https://doi.org/10.1002/2014JC010261

Warden, L., Kim, J. H., Zell, C., Vis, G. J., De Stigter, H., Bonnin, J., & Sinninghe Damsté, J. S. (2016). Examining the provenance of branched GDGTs in the Tagus River drainage basin and its outflow into the Atlantic Ocean over the Holocene to determine their usefulness for paleoclimate applications. *Biogeosciences*, *13*(20), 5719–5738.

Wegner, C., Bennett, K. E., de Vernal, A., Forwick, M., Fritz, M., Heikkilä, M., et al. (2015). Variability in transport of terrigenous material on the shelves and the deep Arctic Ocean during the Holocene. *Polar Research*, *34*(1), 24964. https://doi.org/10.3402/polar.v34.24964

Weijers, J. W. H., Schoten, S., van den Donker, J. C., Hopmans, E. C., & Sinninghe Damsté, J. S. (2007). Environmental controls on bacterial tetraether membrane lipid distribution in soils. *Geochimica et Cosmochimica Acta*, *71*, 703–713.

Yunker, M. B., Backus, S. M., Graf Pannatier, E., Jeffries, D. S., & Macdonald, R. W. (2002). Sources and significance of alkane and PAH hydrocarbons in Canadian Arctic Rivers. *Estuarine, Coastal and Shelf Science*, *55*(1), 1–31.

Yunker, M. B., Macdonald, R. W., Cretney, W. J., Fowler, B. R., & McLaughlin, F. A. (1993). Alkane, terpene and polycyclic aromatic hydrocarbon geochemistry of the Mackenzie River and Mackenzie shelf: Riverine contributions to Beaufort Sea coastal sediment. *Geochimica et Cosmochimica Acta*, *57*(13), 3041–3061.

Yunker, M. B., Macdonald, R. W., Veltkamp, D. J., & Cretney, W. J. (1995). Terrestrial and marine biomarkers in a seasonally ice-covered Arctic estuary—Integration of multivariate and biomarker approaches. *Marine Chemistry*, *49*(1), 1–50.

Guo, L., Ping, C.-L., & Macdonald, R. W. (2007). Mobilization pathways of organic carbon from permafrost to arctic rivers in a changing climate. *Geophysical Research Letters*, *34*, L13603. https://doi.org/10.1029/2007GL030689

Holmes, R. M., McClelland, J. W., Tank, S. E., Spencer, R. G. M., & Shiklomanov, A. I. (2018). Arctic Great Rivers Observatory. Water Quality Dataset, Version 20181010. Retrieved from https://www.arcticgreatrivers.org/data

Hopmans, E. C., Weijers, J. W. H., Schefuß, E., Herfort, L., Sinninghe Damsté, J. S., & Schouten, S. (2004). A novel proxy for terrestrial organic matter in sediments based on branched and isoprenoid tetraether lipids. *Earth and Planetary Science Letters*, *224*(1–2), 107–116.

Schouten, S., Hopmans, E. C., & Sinninghe Damsté, J. S. (2013). The organic geochemistry of glycerol dialkyl glycerol tetraether lipids: A review. *Organic Geochemistry*, *54*, 19–61.

Yunker, M. B., McLaughlin, F. A., Fowler, B. R., Brooks, G., Chiddell, G., Hamilton, C., & Macdonald, R. W. (1992). NOGAP B.6; Volume 9: Hydrocarbon determinations; Mackenzie River and Beaufort Sea. *Canadian Data Repository Hydrography and Ocean Sciences*, *9*(60), 1–294.

References From the Supporting Information

Ascough, P., Cook, G., & Dugmore, A. (2005). Methodological approaches to determining the marine radiocarbon reservoir effect. *Progress in Physical Geography*, *29*(4), 532–547.

Austin, W. E. N., Bard, E., Hunt, J. B., Kroon, D., & Peacock, J. D. (1995). The ^{14}C age of the Icelandic Vedde Ash: Implications for Younger Dryas marine reservoir age corrections. *Radiocarbon*, *37*(1), 53–62.

Blaauw, M., & Christen, J. A. (2011). Flexible paleoclimate age-depth models using an autoregressive gamma process. *Bayesian Analysis*, *6*(3), 457–474.

Meyer, V. D., Max, L., Hefter, J., Tiedemann, R., & Mollenhauer, G. (2016). Glacial-to-Holocene evolution of sea surface temperature and surface circulation in the subarctic northwest Pacific and the Western Bering Sea. *Paleoceanography*, *31*, 916–927. https://doi.org/10.1002/2015PA002877

Reimer, P. J., Bard, E. B., Bayliss, A., Beck, J. W., Blackwell, P. G., Ramsey, C. B., et al. (2013). Intcal13 and Marine13 radiocarbon age calibration curves 0–50,000 years cal BP. *Radiocarbon*, *55*(4), 1869–1887. https://doi.org/10.2458/azu_js_rc.55.16947

Rethemeyer, J., Fülöp, R. H., Höfle, S., Wacker, L., Heinze, S., Hajdas, I., et al. (2013). Status report on sample preparation facilities for ^{14}C analysis at the new CologneAMS center. *Nuclear Instruments and Methods in Physics Research, Section B: Beam Interactions with Materials and Atoms*, *294*, 168–172. https://doi.org/10.1016/j.nimb.2012.02.012

Schouten, S., Huguet, C., Hopmans, E. C., Kienhuis, M. V. M., & Sinninghe Damsté, J. S. (2007). Analytical methodology for TEX86 paleothermometry by high-performance liquid chromatography/atmospheric pressure chemical ionization-mass spectrometry. *Analytical Chemistry*, *79*(7), 2940–2944.

Synal, H.-A., Stocker, M., & Suter, M. (2007). MICADAS: A new compact radiocarbon AMS system. *Nuclear Instruments and Methods in Physics Research, Section B: Beam Interactions with Materials and Atoms*, *259*(1), 7–13.

Wacker, L., Christl, M., & Synal, H. A. (2010). Bats: A new tool for AMS data reduction. *Nuclear Instruments and Methods in Physics Research, Section B: Beam Interactions with Materials and Atoms*, *268*(7–8), 976–979.

Wacker, L., Němec, M., & Bourquin, J. (2010). A revolutionary graphitisation system: Fully automated, compact and simple. *Nuclear Instruments and Methods in Physics Research, Section B: Beam Interactions with Materials and Atoms*, *268*(7–8), 931–934.

Wenger, L. M., & Isaksen, G. H. (2002). Control of hydrocarbon seepage intensity on level of biodegradation in sea bottom sediments. *Organic Geochemistry*, *33*(12), 1277–1292.